Endothelial Cell–Dependent Regulation of Arteriogenesis

Filipa Moraes, Julie Paye, Feilim Mac Gabhann, Zhen W. Zhuang, Jiasheng Zhang, Anthony A. Lanahan and Michael Simons

Circ Res. 2013;113:1076-1086; originally published online July 29, 2013;
doi: 10.1161/CIRCRESAHA.113.301340
Circulation Research is published by the American Heart Association, 7272 Greenville Avenue, Dallas, TX 75231

Print ISSN: 0009-7330. Online ISSN: 1524-4571

Endothelial Cell–Dependent Regulation of Arteriogenesis

Filipa Moraes, Julie Paye, Feilim Mac Gabhann, Zhen W. Zhuang, Jiasheng Zhang, Anthony A. Lanahan, Michael Simons

Rationale: **Arteriogenesis is the process of formation of arterial conduits. Its promotion is an attractive therapeutic strategy in occlusive atherosclerotic diseases. Despite the functional and clinical importance of arteriogenesis, the biology of the process is poorly understood. Synectin, a gene previously implicated in the regulation of vascular endothelial cell growth factor signaling, offers a unique opportunity to determine relative contributions of various cell types to arteriogenesis.**

Objective: **We investigated the cell-autonomous effects of a synectin knockout in arterial morphogenesis.**

Methods and Results: **A floxed synectin knockin mouse line was crossbred with endothelial-specific (Tie2, Cdh5, Pdgfb) and smooth muscle myosin heavy chain–specific Cre driver mouse lines to produce cell type–specific deletions. Ablation of synectin expression in endothelial, but not smooth muscle cells resulted in the presence of developmental arterial morphogenetic defects (smaller size of the arterial tree, reduced number of arterial branches and collaterals) and impaired arteriogenesis in adult mice.**

Conclusions: **Synectin modulates developmental and adult arteriogenesis in an endothelial cell–autonomous fashion. These findings show for the first time that endothelial cells are central to both developmental and adult arteriogenesis and provide a model for future studies of factors involved in this process. (*Circ Res*. 2013;113:1076-1086.)**

Key Words: arteries ■ arteriogenesis ■ collateral ■ endothelial cells ■ receptors ■ synectin ■ vascular endothelial growth factor

Arteriogenesis, the process of formation of arterial conduits, is a promising therapeutic approach for the treatment of several ischemic vascular diseases. Yet, its biology remains poorly understood. New vasculature can form via 3 distinct processes: vasculogenesis, angiogenesis, and arteriogenesis. Vasculogenesis refers to the formation of the primitive vascular plexus from vascular progenitor cells during embryonic development. Angiogenesis is the process of new capillary formation that occurs by sprouting or longitudinal splitting (intussusception) of existing vessels.[1,2] Finally, arteriogenesis refers to the development of larger vessels such as arterioles and arteries.[3] Collateral formation represents a specific case of arteriogenesis. By definition, collateral vessels provide artery-to-artery connections and are thought to play a protective role by providing alternative routes to blood flow.[4,5]

In This Issue, see p 1033

Although angiogenesis is largely driven by vascular endothelial growth factor (VEGF) production in response to hypoxia[6] or inflammation,[2] little is known about factors controlling arteriogenesis, in general, and collateral formation, in particular. In adult tissues, arteriogenesis can occur at sites of arterial occlusion where ischemia is not prominent and is thought to be triggered by hemodynamic factors, such as changes in shear stress forces sensed by endothelial cells (ECs).[7,8] How that happens is the subject of considerable controversy. One possible scenario is that arteriogenesis is the result of remodeling of preexisting collaterals. The existence of small collaterals that expand on occlusion of the main arterial trunk has been clearly described, both in animals[9] and in humans,[10] and the ability to restore compromised tissue perfusion has been linked to the extent of preexisting collateral circulation.[11]

Alternatively, adult arteriogenesis has been described as a de novo process that occurs by the expansion and arterialization of the capillary bed.[12–14] In this scenario, the ability of ECs to proliferate and secrete growth factors, is crucial for new vascular network development and subsequent arterialization via recruitment of mural cells. One piece of evidence strongly in favor of this hypothesis is the extent of new arterial growth observed by micro-computed tomographic (mCT) angiography after a large artery occlusion.[15] This is highly unlikely to arise solely from preexisting collaterals.

Studies during the past decade have identified several growth factors, including platelet-derived growth factor (PDGF)

Original received March 9, 2013; revision received July 25, 2013; accepted July 29, 2013. In June 2013, the average time from submission to first decision for all original research papers submitted to *Circulation Research* was 13.67 days.

From the Department of Internal Medicine, Yale Cardiovascular Research Center, Section of Cardiovascular Medicine, New Haven, CT (F.M., Z.W.Z., J.Z., A.A.L., M.S.); Dartmouth College, Hanover, NH (J.P.); Institute for Computational Medicine and Department of Biomedical Engineering, Johns Hopkins University, Baltimore, MD (F.M.G.); and Department of Cell Biology, Yale University School of Medicine, New Haven, CT (M.S.).

The online-only Data Supplement is available with this article at http://circres.ahajournals.org/lookup/suppl/doi:10.1161/CIRCRESAHA.113.301340/-/DC1.

Correspondence to Michael Simons, MD, Cardiovascular Medicine, Yale University School of Medicine, PO Box 802017, 333 Cedar St, New Haven, CT 06520-2017. E-mail michael.simons@yale.edu

Nonstandard Abbreviations and Acronyms

EAA1	early endosome antigen 1
EEA1	early endosomal antigen 1
EC	endothelial cell
ECKO	endothelial cell knockout
ERK	extracellular response kinase
iEC-SynKO	induced endothelial synectin knockout
mCT	micro-computed tomography
PDZ	protein interaction domain, named after a common structure found in PSD-95, discs large, and zona occludens 1 proteins
SMC	smooth muscle cell
SMKO	smooth muscle cell knockout
VEGF	vascular endothelial cell growth factor

fibroblast growth factors, and VEGF,[16–20] cytokines such as monocyte chemotactic protein 1,[21,22] peptides such as neuropeptide Y,[23] and master regulators such as hypoxia-inducible factor-1α,[24,25] hypoxia-inducible factor-2α,[26] and PR39[27,28] that can promote arteriogenesis. Of these, VEGF-A seems to play the central role. In particular, experimental studies have demonstrated that collateral growth is prevented by anti–VEGF-A—neutralizing antibodies,[5] VEGF receptor (VEGFR) inhibitors,[29] and soluble VEGFR traps,[30] whereas genetic approaches further demonstrated the requirement for VEGF-A expression for collateral development in healthy tissue.[17] Disruption of VEGF signaling as a result of impairment of VEGFR2 trafficking has also been shown to result in decreased arteriogenesis.[31–33]

Although the role of VEGF-A in arteriogenesis is well-established, its cellular site of action remains uncertain. In this study, we set out to address the cellular underpinnings of VEGF-dependent arteriogenesis. To this end, we have taken advantage of the recent identification of an arterial morphogenetic defect associated with a global deletion of synectin by our laboratory.[31,32] Synectin is a widely expressed single PDZ domain protein that interacts with a variety of plasma membrane and cytoplasmic molecules[31,34,35] to control intracellular signaling. Homozygous disruption of synectin in mice or a knockdown of its expression in zebrafish results in a selective reduction of arterial morphogenesis, including decreased branching and reduced size and diameter of the arterial vasculature.[31] Synectin-null ECs have reduced responsiveness to VEGF stimulation[31,32] and decreased activation of ERK, whereas their responses to other growth factors such as fibroblast growth factors and insulin-like growth factor are normal.[32] In addition, synectin-null mice display downregulation of PDGF expression in the endothelium, likely accounting for the loss of vascular smooth muscle cell (SMC) coverage of smaller blood vessels observed in these settings.[36] This gene, therefore, offers a unique ability to help determine relative contributions of various cell types to arteriogenesis.

To study that problem, we generated a mouse line with a floxed synectin gene knocked-in into the synectin (*gipc1*) locus and crossbred it with endothelial (Tie2, Cdh5, and Pdgfb) and smooth muscle myosin heavy chain–specific Cre mouse lines to produce EC-specific and SMC-specific deletions, respectively. We found that ablation of synectin expression in EC but not SMC mimicked the arterial phenotype of global synectin-null mutants,[31] thereby implicating endothelium as the key cell type regulating arteriogenesis.

Methods

Full methods are described in the online-only Data Supplement.

Mice

Mice homozygous for a conditional allele of synectin (*gipc1*) were generated by flanking exon 2 with *loxP* sites. Exon 2 of synectin

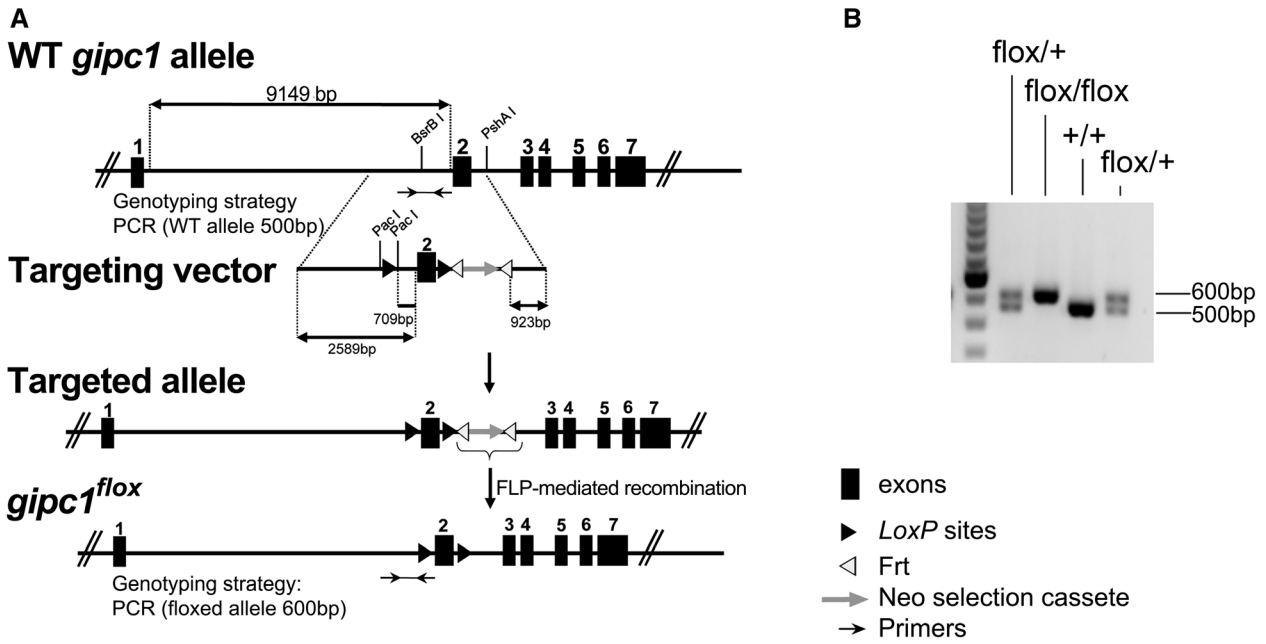

Figure 1. Generation of a floxed allele of the mouse synectin gene. A, The targeting vector contains a loxP site (black triangle) into *Bsr*BI restriction site upstream of exon 2, exon 2 cDNA, a fragment with neo selection cassette (gray arrow), and a loxP site into the *Psh*AI site downstream of exon 2. The Frt-flanked neo cassette was removed by flipase (Flp)-mediated site-specific recombination (Frt recombination elements are indicated by white triangles). **B**, Genomic mouse DNA was genotyped with the oligonucleotides indicated in (**A**) (black arrows). PCR indicates polymerase chain reaction; and WT, wild type.

(*gipc1*) was deleted by crossing the *gipc1*$^{flox/flox}$ mice with smooth muscle myosin heavy chain-Cre,[37] Tie2-Cre,[38] Cdh5-CreERT2,[39] or Pdgfb-Cre/ERT2[40] mice. All animal experiments were performed under a protocol approved by the Institutional Animal Care and Use Committee of Yale University.

Primary SMC and EC Isolation and Culture

Primary SMCs were isolated from dorsal aorta, as previously described,[41] with minor modifications. Primary ECs were isolated from the heart and lung of adult mice using a previously described protocol.[31]

Hindlimb Ischemia Model

The hindlimb ischemia model was performed as previously described in our laboratory.[28,31] Laser Doppler flow imaging was performed using a Moor Infrared Laser Doppler Imager (Moor Instruments) at 36.5°C to 37.5°C under isoflurane anesthesia.

Micro-CT Angiography

mCT of the cardiac, renal, and hindlimb vasculature was performed by injecting 0.7 mL bismuth contrast solution in the descending aorta, and the vasculature was imaged and quantified as described previously.[28,31,42]

Spinotrapezius Assay

Spinotrapezius muscles (both left and right) from euthanized mice were stripped of fascia and dissected as described previously.[14,43] Quantifications of vessel diameters and collateral arcades were performed using ImageJ software.[44]

Retina Analysis

The eyes were harvested at postnatal day 5 and postnatal day 17 and processed as described in the online-only Data Supplement.

In Vivo Matrigel Assay

The Matrigel was premixed with heparin (5 U) with or without VEGF-A_{165} (100 ng/mL) and injected subcutaneously. Seven days later, the plugs were recovered from the euthanized mice, embedded in optimum cutting temperature compound, cryosectioned in 10-μm sections, and stained with anti-CD31 antibody.

Wound Healing Assay

Wound healing assays were performed by creating 6-mm punch wounds in the skin of the back of 12-week to 14-week-old male mice. The healing process was analyzed over time.[45]

Results

Generation of *gipc1* Floxed Mice and Smooth Muscle and Endothelial Knockouts

To evaluate the specific contributions of ECs and SMCs to arteriogenesis, we generated mice carrying a floxed synectin allele inserted into the endogenous *gipc1* gene locus. The targeting strategy (Figure 1A) resulted in the creation of a *gipc1* allele, with *loxP* sites flanking a neomycin resistance cassette and exon 2 of the *gipc1* gene. The neomycin resistance gene was subsequently

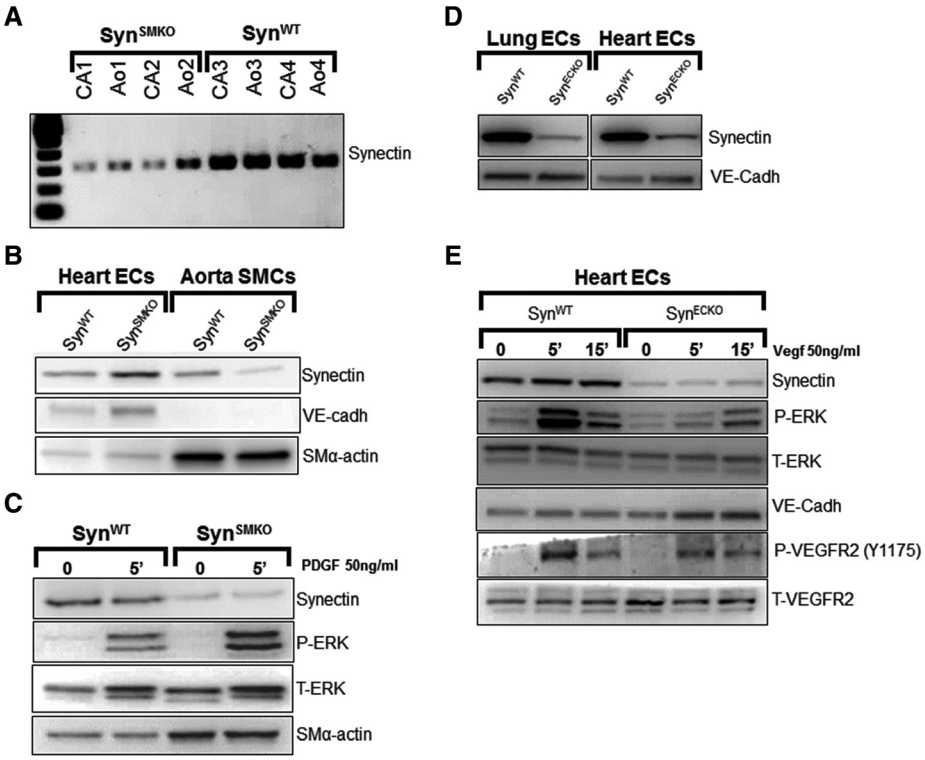

Figure 2. Validation of Syn^{SMKO} and Syn^{ECKO} mouse lines. A–C, In vivo ablation of synectin expression in smooth muscle cells (Syn^{SMKO}). **A**, Decreased synectin RNA levels in carotid (CA) and aorta (Ao) from Syn^{SMKO} mice compared with control littermates. **B**, Western blot of total cell lysates of aortic smooth muscle cells (SMCs) and heart endothelial cells (ECs) from Syn^{SMKO} mice. Note a reduction in synectin protein levels in SMCs but not in ECs. **C**, ERK activation. Western blot analysis of total cell lysate of aortic SMC. Confluent, serum-starved cells were stimulated for 5 minutes with 50 ng/mL platelet-derived growth factor (PDGF)-BB. Phosphorylation of ERK (P-ERK) in response to PDGF-BB is not altered in synectin-null SMCs (Syn^{SMKO}) relative to wild-type SMCs (Syn^{WT}). **D** and **E**, In vivo ablation of synectin expression in endothelial cells (Syn^{ECKO}). **D**, Decreased synectin protein levels in ECs isolated from Syn^{ECKO} mice compared with Syn^{WT} mice. **E**, Western blotting of total cell lysates isolated from heart ECs. Confluent, serum-starved ECs were stimulated for the times indicated with 50 ng/mL vascular endothelial growth factor (VEGF)-A_{165}. Note reduced P-ERK and phosphorylation of VEGFR2 Y1175 site (P-VEGFR2 Y1175) in synectin-null endothelial cells. ECKO indicates endothelial cell conditional knockout; P-VEGFR2, phosphorylated VEGFR2; SM-α-actin, SMC α-actin; SMKO, smooth muscle cell conditional knockout; Syn, synectin; T-ERK, total ERK; T-VEGFR2, total VEGFR2; VE-cadh, vascular endothelial cadherin; and WT, wild-type.

removed using *flp*-mediated recombination. Screening of the progeny confirmed the presence of the floxed allele (Figure 1B).

To ablate synectin expression in SMCs, *gipc1*$^{fl/fl}$ mice were crossed with smooth muscle myosin heavy chain-Cre strain, and the progeny were bred to produce mice homozygous for the loss of smooth muscle synectin expression (Syn^{SMKO}). Genotyping of litters containing Syn^{SMKO} mice (smooth muscle myosin heavy chain-Cre;Syn^{FF}) revealed the presence of all genotypes with the expected Mendelian frequency.

Carotid arteries and aorta from Syn^{SMKO} mice had markedly lower mRNA levels of synectin than littermate controls (Figure 2A). Western blot analysis of synectin expression in primary SMCs and ECs, isolated from these mice, confirmed nearly complete loss of synectin expression in SMCs but not in ECs (Figure 2B). Stimulation of Syn^{SMKO} SMCs with PDGF-BB, one of the key growth factors regulating SMC migration and proliferation, revealed no differences in ERK activation compared with control SMCs, demonstrating that synectin expression in smooth muscle is not required for a normal response to PDGF-BB stimulation (Figure 2C). These observations are in line with what has been previously shown in SMCs from global synectin-null mice.[36]

To ablate synectin in EC, homozygous floxed synectin mice were crossed with the Tie2-Cre mouse line and the progeny were bred for endothelial-specific knockout of synectin (Syn^{ECKO}). Western blot analysis of primary heart and lung ECs isolated from these mice confirmed a marked reduction in synectin expression in these cells (Figure 2D). Previous studies from our laboratory have demonstrated reduced responsiveness to VEGF stimulation of synectin-null arterial EC isolated from synectin global knockout mice.[31,32] To confirm that EC-selective disruption of synectin resulted in the same phenotype at the cellular level, we examined VEGF signaling in ECs isolated from Syn^{ECKO} mice. Analysis of VEGFR2 activation after stimulation with VEGF-A demonstrates an expected reduction in Y^{1175} site phosphorylation and a decrease in ERK1/2 activation (Figure 2E).

Impaired Arterial Development in Syn^{ECKO} But Not in Syn^{SMKO} Mice

To assess the impact of EC and SMC synectin deletion in the arterial development, we performed mCT angiography of the heart (Figure 3A) and renal vasculature (Figure 3B) of Syn^{SMKO}, Syn^{ECKO}, and littermate control mice as described previously.[28,31]

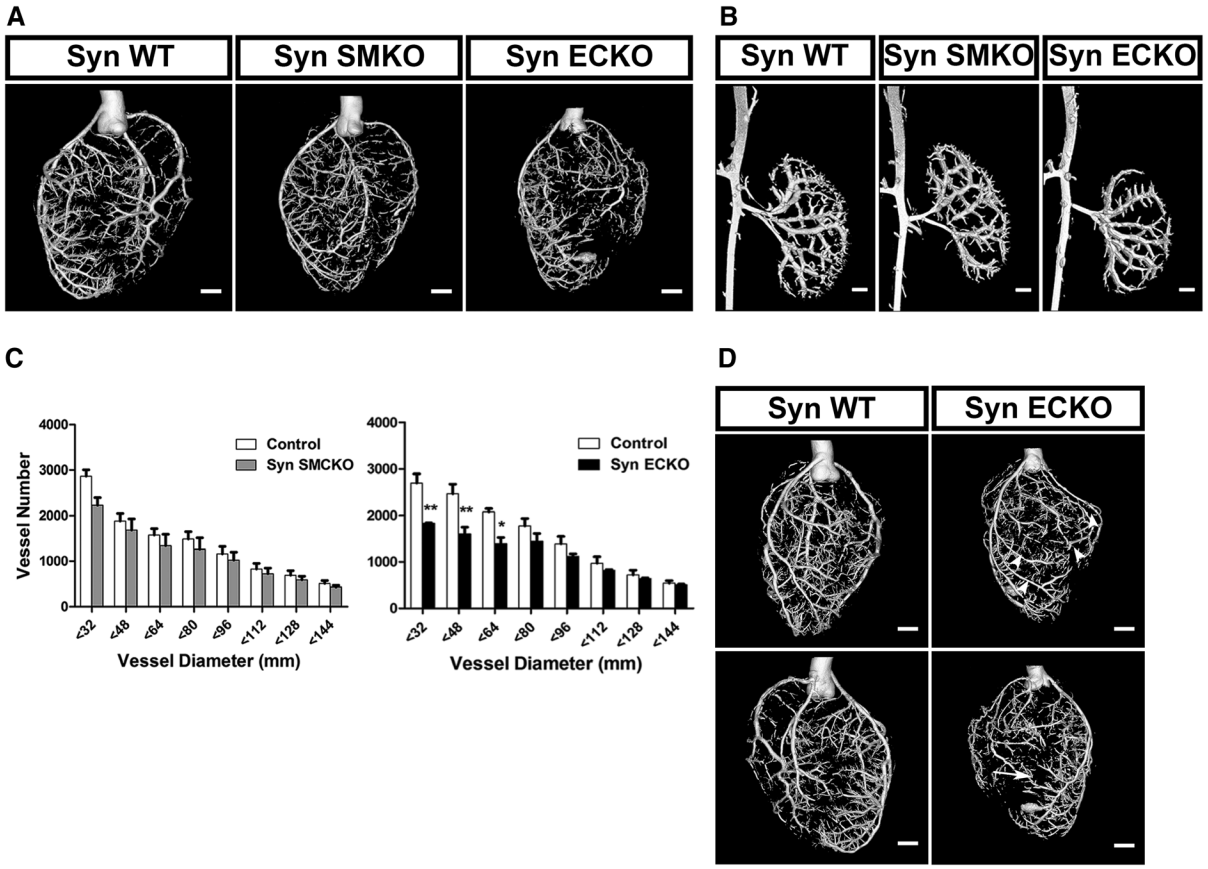

Figure 3. Developmental arteriogenesis defects are present in Syn^{ECKO} but not in Syn^{SMKO} mice. Representative reconstructed micro-computed tomographic (mCT) images of whole heart (**A**) and kidney (**B**) arterial vasculature (16-μm resolution; n=4) from age-matched and sex-matched Syn^{WT}, Syn^{SMKO}, and Syn^{ECKO} mice. Note marked reduction in branching in Syn^{ECKO} mice compared with Syn^{SMKO} or Syn^{WT} control mice. **C**, Quantitative analysis of mCT images of whole hearts (gray bars, Syn^{SMKO}; black bars, Syn^{ECKO}). Note a marked decrease in the total number of <64-μm-diameter arterial vessels in Syn^{ECKO} mice relative to control littermates (F=3.962, P=0.003; post hoc Tukey honestly significant difference test: *P<0.01; **P<0.001). **D**, Reconstructed mCT images of the heart vasculature from Syn^{ECKO} mice. Note the presence of aneurism-like structures (arrow) and increased diameters in the distal part of some arteries compared with their proximal part (arrowheads). Scale bar, 1 mm. ECKO indicates endothelial cell conditional knockout; SMKO, smooth muscle cell conditional knockout; Syn, synectin; and WT, wild-type.

Arterial trees in both the heart and kidneys of Syn^{ECKO}, but not Syn^{SMKO}, mice exhibited less branching, had fewer artery-to-artery connections (collateral arteries), and appeared smaller in diameter. Quantitative analysis of coronary circulation showed a significant decrease in the number of smaller arteries (≤64 μm in diameter) in Syn^{ECKO} mice. Syn^{SMKO} mice showed a trend toward reduced number of smaller arteries (≤32 μm in diameter), which was not statistically significant (Figure 3C). This reduction in the number of smaller-caliber arteries in Syn^{ECKO} mice is similar to that observed in the global synectin knockout.[31] To our surprise, we found aneurysmal dilations of distal coronary arteries (Figure 3D, arrowheads) and even frank tubular aneurysms in Syn^{ECKO} mice (arrow) that were not previously seen in global synectin-null mice.

To gain a better understanding of arterial microcirculation changes associated with an endothelial-specific synectin knockout, we examined vascular networks in the spinotrapezius muscle.[14] Because of its thinness (≈150 μm), the entire vascular network of the muscle can be imaged in whole-mount at micron-level resolution (Figure 4A). The muscle is fed by multiple arterioles, notably lateral and caudal feed vessels (Figure 4A, red arrowheads) that are connected by an arteriolar arcade network providing multiple collateral pathways for blood flow.[14,46] In wild-type mice, the collateral networks have a ramified arcade structure with multiple arteriole linkage, whereas in Syn ^{ECKO} mice the network has a dendritic structure with smaller arteries and fewer arteriolar-level connections (Figure 4A). No abnormalities were observed in Syn^{SMKO} mice (images not shown). This finding was confirmed by quantitative analysis of the spinotrapezius circulation in wild-type, Syn^{ECKO}, and Syn^{SMKO} mice (Figure 4B and 4C). The input arterioles are significantly narrower in the Syn^{ECKO} but not Syn^{SMKO} mice compared with littermate controls (Figure 4B), thus confirming spinotrapezius angiography and coronary mCT observations. In addition, the number of arteriolar arcades (collateral arteries) is significantly lower in Syn^{ECKO} compared with Syn^{SMKO} or littermate control mice (Figure 4C).

Postnatal Arteriogenesis Defects in Synectin Endothelial Knockout Mice

To investigate the effect of SMC-specific and EC-specific synectin knockout on arterial morphogenesis in adult tissues, we next analyzed arteriogenesis in Syn^{SMKO} and Syn^{ECKO} mice using a hindlimb ischemia model. In this model, arteriogenesis is induced by ligation and excision of a segment of the common femoral artery of 10-12 week old mice.[28] After artery ligation, blood flow in the distal limb is assessed by a deep-penetrating laser Doppler and expressed as a ratio of flow in the foot of operated to nonmanipulated limb. Immediately after surgery, there was a dramatic but equal reduction in perfusion in all 3 groups (Figure 5A and 5D). Blood flow in the distal limb of control and Syn^{SMKO} mice recovered to the same extent during the next 2 weeks (Figure 5A). Because growth of new arterial vasculature is the principal event responsible for blood flow restoration in this model, we next performed mCT analysis to visualize and quantify the extent of hindlimb vasculature 14 days after surgery. In agreement with the finding of unimpaired distal blood flow recovery, mCT of the arterial vasculature confirmed comparable arteriogenesis in Syn^{SMKO} and

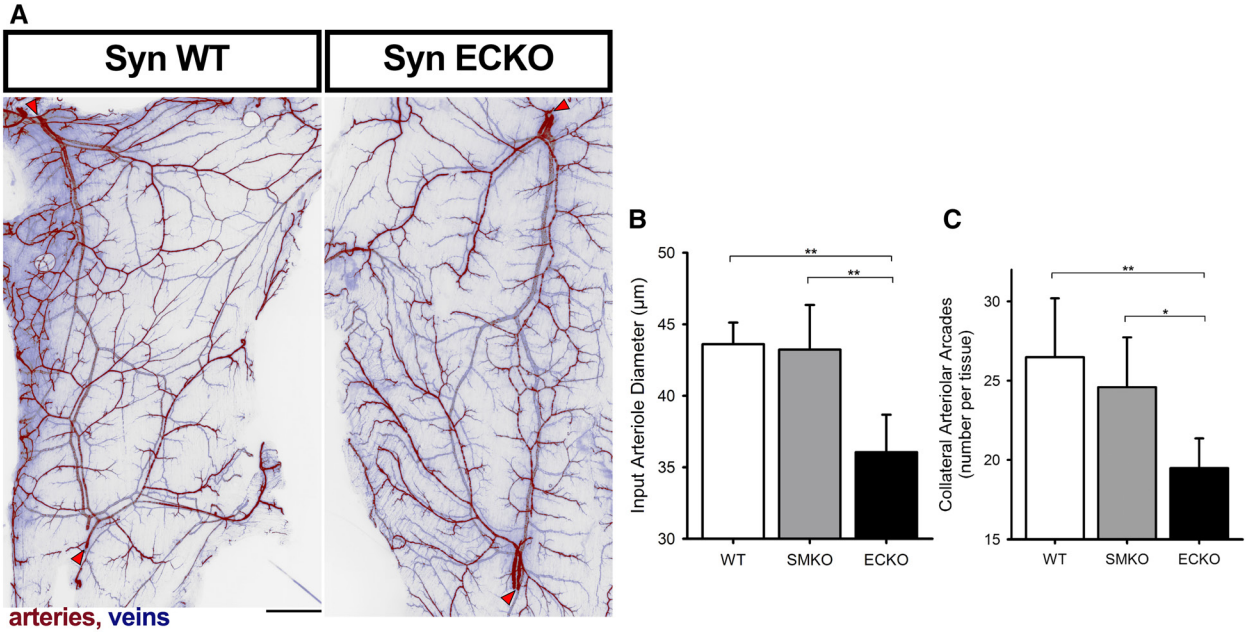

Figure 4. Quantification of arterial networks in mouse skeletal muscle. A, Fluorescent image of the caudal half of the mouse spinotrapezius. Pseudocoloring is used to indicate arteries (red) and veins (blue). Scale bar, 500 μm. Input arterioles entering the muscle are denoted by red arrowheads. Note extensive arcading arterial networks providing collateral pathways between the lateral (top left) and caudal (bottom left) input arterioles. The networks of spinotrapezius muscle vasculature in controls (Syn^{WT}) have a ramified arcade structure, with multiple arteriole linkage. Note that networks in Syn^{ECKO} mice have a predominantly dendritic structure with few arteriolar-level connections. **B**, Diameter of the input arterioles as they enter the spinotrapezius. **C**, Number of arcades in the caudal collateral spinotrapezius arterial network. Wild-type mice, n=10; Syn^{SMKO} and ^{ECKO} mice, n=6. ANOVA with Tukey honestly significant difference post hoc test analysis: *P<0.05; **P<0.01. ECKO indicates endothelial cell knockout; SMKO, smooth muscle cell knockout; Syn, synectin; and WT, wild-type.

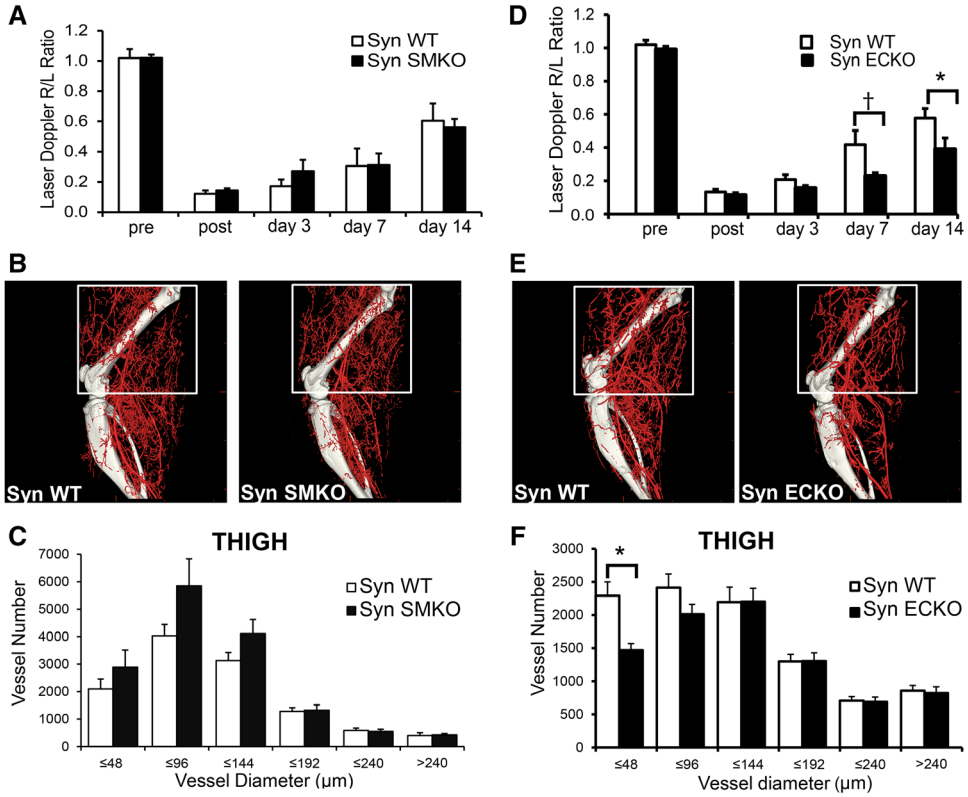

Figure 5. Impaired blood flow recovery in Syn^{ECKO} mice after ligation of femoral artery. Laser Doppler analysis of blood flow perfusion. Syn^{SMKO} (**A**) and Syn^{ECKO} (**D**) mice were subjected to common femoral artery ligation. The graph shows blood flow in the ischemic foot (**right**) expressed as a ratio of flow in the normal foot (left; R/L) at various time points after femoral artery ligation. Note the absence of flow recovery in Syn^{ECKO} mice at 7 and 14 days. Mean±SD, **P*<0.05, †*P*=0.07 (n=10 per group). Representative micro-computed tomographic (mCT) images of reconstructed limb arterial vasculature from Syn^{SMKO} (**B**) and Syn^{ECKO} (**E**) mice compared with control littermates 14 days after surgery. Quantitative mCT analysis in Syn^{SMKO} (**C**) and Syn^{ECKO} (**F**) mice compared with control littermates. Note a significant decrease in the amount of smaller size arteries in Syn^{ECKO} mice compared with control group (C) (**P*<0.05; n=5 mice/group). ECKO indicates endothelial cell knockout; SMKO, smooth muscle cell knockout; Syn, synectin; and WT, wild-type.

wild-type mice (Figure 5B and 5C). Interestingly, there was a nonsignificant trend toward larger artery sizes in Syn^{SMKO} but not in control mice (Figure 5C). However, blood flow recovery was significantly impaired in Syn^{ECKO} mice, which was apparent 1 week after surgery (Figure 5D) and was similar to that previously observed in synectin global knockout mice. As expected, mCT analysis of the arterial circulation demonstrated a significant reduction in the number of smaller arterial vessels in the tight muscle (Figure 5E and 5F).

Inducible Ablation of Synectin Expression in ECs

Because the Tie2 promoter has been shown to activate Cre expression not only in endothelial lineage but also in hematopoietic lineages during development,[47] this may result in deletion of synectin expression in monocytes and monocyte-derived macrophages. These cells play an important role in postnatal arteriogenesis, particularly in the hindlimb ischemia model.[48,49] To exclude the possibility that decreased synectin expression in cells other than the endothelium was responsible for the impaired arteriogenesis after common femoral artery ligation in adult mice, we used *Cdh5-CreERT2* transgenic mouse line.[39] Unlike Tie2, Cdh5 expression is much more restricted to the endothelium, and little, if any, expression occurs in cells of hematopoietic lineages postnatally.

Analysis of the arteriogenesis in the hindlimb ischemia model was performed in 10-week-old sex-matched induced endothelial synectin knockout (iEC-SynKO) mice and controls (n=6/group). Similar to Syn^{ECKO} (Tie2-Cre;Syn^{FF}), iEC-SynKO (Cdh5-CreERT2;Syn^{FF}) mice demonstrated a significant decline in blood flow recovery after the common femoral artery ligation (Figure 6A and 6B). Quantitative polymerase chain reaction analysis of synectin mRNA expression in lung ECs isolated from iEC-SynKO mice (n=3) showed markedly decreased expression compared with controls (Figure 6C).

Analysis of the spinotrapezius vascular networks in iEC-SynKO mice again demonstrated a significant reduction in the number of collateral arcade structures compared with control littermates (Figure 6D and 6E). In addition, diameters of the input arterioles were significantly less in iEC-SynKO mice compared with control littermates (Figure 6E), similar to what was observed in Syn^{ECKO} mice.

To assess the impact of reduced endothelial synectin expression in angiogenesis, we analyzed postnatal day 5 and postnatal day 17 retinas from Tie2-Cre;Syn^{FF} (Syn^{ECKO}) mice (Figure 7A) and postnatal day 5 retinas from Pdgfb-iCre/ERT2;Syn^{FF} mice (Figure 7B) induced on the first postnatal day. Retinal angiogenesis included the extent of vascular coverage, and the number of vascular branch points was similar in synectin mutant lines and in their littermate controls.

To address the effect of synectin ablation on adult angiogenesis, we first used a puncture wound model in

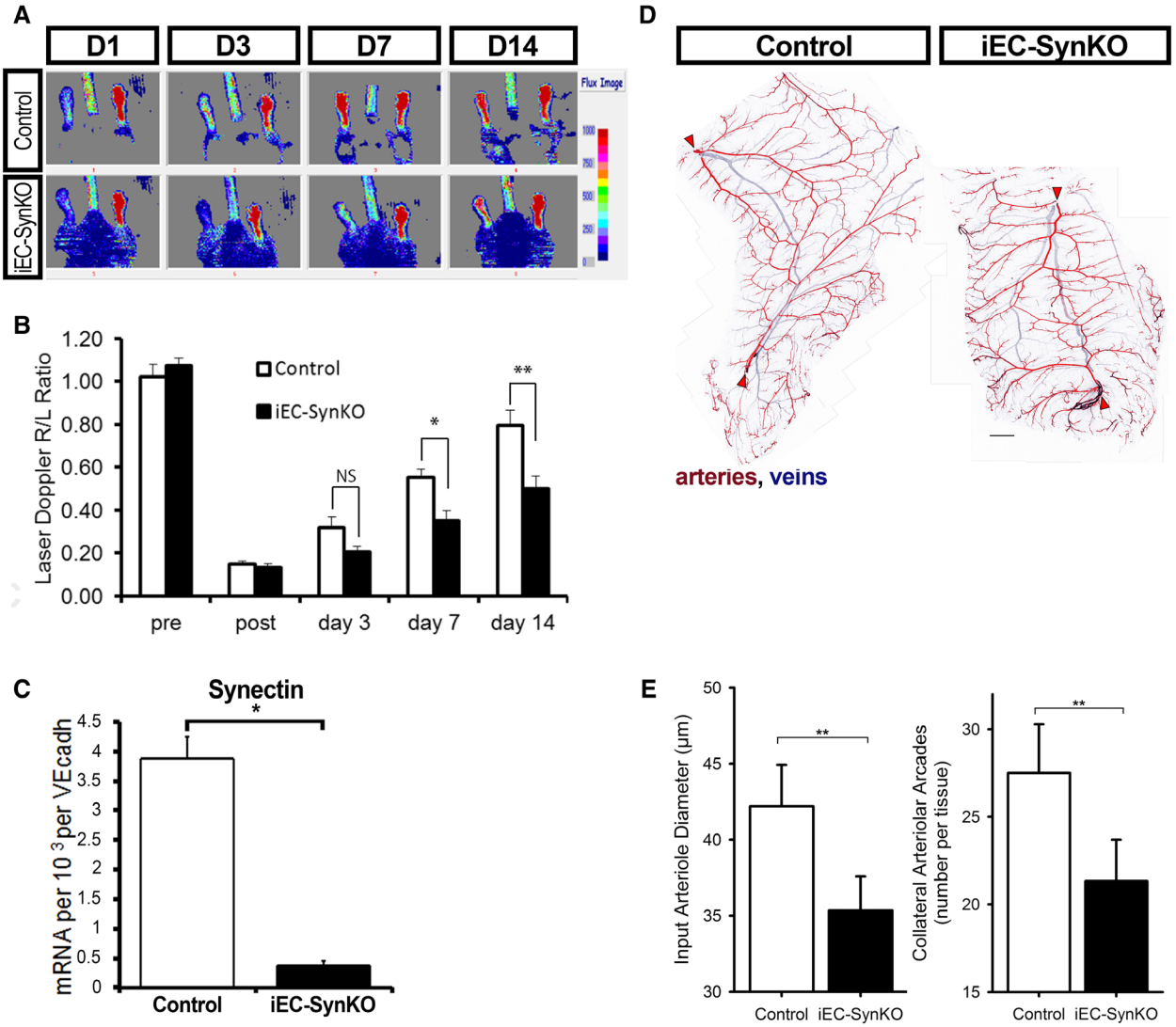

Figure 6. Arteriogenesis defects in induced endothelial synectin knockout (iEC-SynKO) mice. A and **B**, Laser Doppler analysis of blood flow perfusion in iEC-SynKO (Cdh5-CreERT2;Syn^{FF}) and control mice subjected to common femoral artery ligation. **B**, Laser Doppler analysis of blood flow recovery after surgery expressed as a ratio of flow in ischemic (R) to normal (L) foot (R/L ratio) at various time points. Note a significant decrease in flow recovery in iEC-SynKO mice at 7 and 14 days compared with controls. Mean±SD, *P≤0.05, **P≤0.01 (n=6 per group). **C**, Decreased synectin RNA levels in lung endothelial cells (ECs) from iEC-SynKO mice compared with control. **D**, Image of the caudal half of the mouse spinotrapezius. Staining for smooth muscle α-actin has been pseudocolored to indicate arteries (red) and veins (blue). Scale bar, 500 μm. Input arterioles entering the muscle are denoted by red arrowheads. **E**, Quantitative analysis of the number of collateral arcades in the spinotrapezius muscle and diameter of the input arterioles as they enter the muscle in iEC-SynKO and wild-type (WT) mice (n=3 each); P≤0.05, 2-tailed t test. Syn indicates synectin; and VE-cadh, vascular endothelial cadherin.

Cdh5Cre-ERT2;Syn^{FF} mice (iEC-SynKO). The rate of wound healing in this model reflects the underlying angiogenesis, and angiogenic defects impair the rate of wound closure.[45] Visual inspection and quantitative analysis demonstrated no difference in wound closure rate between synectin deletants and littermate controls (Figure 8A and 8B). Finally, iEC-SynKO mice were used for an in vivo Matrigel assay. Analysis of Matrigel plugs impregnated with VEGF extracted from control and iEC-SynKO mice demonstrated no differences (Figure 8C and 8D).

Discussion

The results of this study demonstrate that synectin modulates developmental and adult arteriogenesis in an EC-autonomous fashion. In addition, we demonstrate that endothelial synectin is not required for adult angiogenesis. Specifically, synectin knockout in EC results in several developmental and adult arterial morphogenetic defects, including smaller size of the arterial tree, reduced numbers of arterial branches and collaterals, and impaired blood flow recovery after common femoral artery ligation. At the same time, SMC-specific deletion of synectin does not affect the size of the arterial tree, the number of collaterals, or blood flow recovery in adult animals.

We focused on cell type–specific synectin knockout because of its critical role in the regulation of VEGF signaling, which is central to the process of arteriogenesis.[50] Synectin accomplishes this by facilitating, in complex with myosin VI, trafficking of newly endocytosed VEGFR2-containing vesicles away from the plasma membrane to EEA1^{+} endosomes. This allows prolonged phosphorylation of the VEGFR2 Y^{1175} site involved in the activation of PLCγ/ERK signaling, which is essential for normal

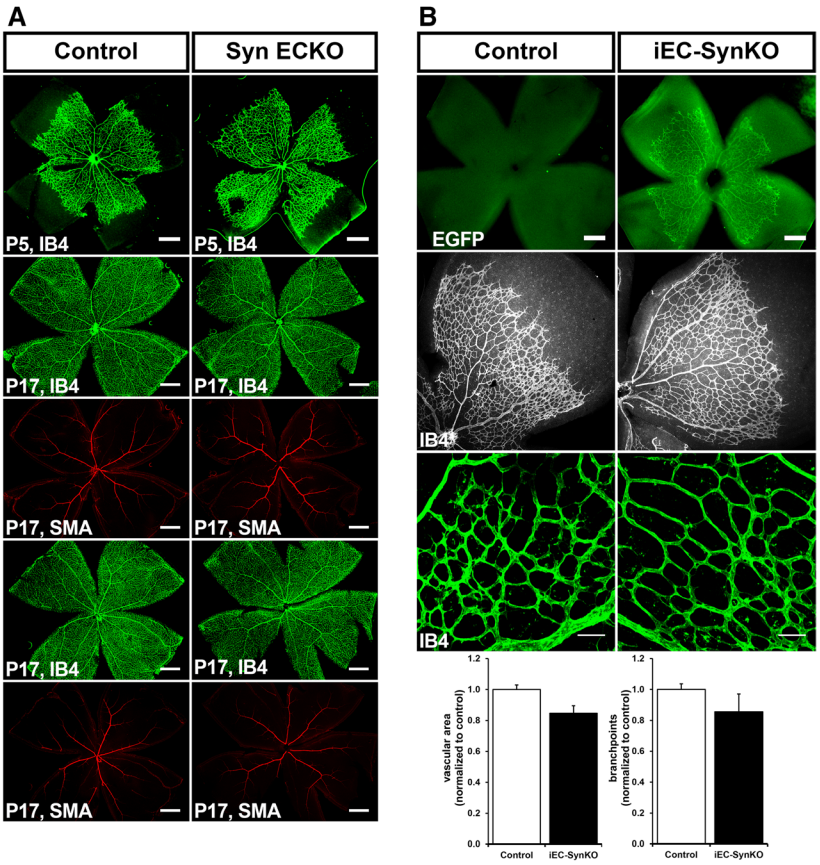

Figure 7. Retinal angiogenesis is not affected in Syn^{ECKO} and induced endothelial synectin knockout (iEC-SynKO) mouse lines. A, Whole mounts of postnatal day (P) 5 and P17 retinas from Syn^{ECKO} mice labeled with isolectin B4 (IB4) and stained with smooth muscle α-actin (SMA) antibody. Representative images for P5 (**top**) and P17 (2, **bottom**) are shown. There were no visual differences in vessel area and SMC coverage between Syn^{ECKO} mutants and controls. Scale bar, 0.5 mm (n=4 mice/group). **B**, Quantitative analysis of P5 whole-mount retinas from iEC-SynKO mice generated with Pdgfb-iCre. Expression of enhanced green fluorescent protein (EGFP) in mutant pups demonstrates the efficiency of Cre induction after tamoxifen administration (**top**; scale bar, 200 μm). Retinal vasculature and quantitative analysis of vascular area and vessel branch points are shown (**bottom**; scale bar, 50 μm; n=3 mice/group). ECKO indicates endothelial cell conditional knockout; and Syn, synectin.

arteriogenesis.[51] Although this mechanism has been shown to operate in ECs, given the ubiquitous nature of synectin expression and the central role of synectin/myosin VI complex in trafficking intracellular vesicles formed during clathrin-dependent endocytosis,[52] it is possible that the same holds true in all cells expressing VEGF receptors.

To address the cell-autonomous effects of synectin, we used SMC-specific and EC-specific Cre driver lines crossed with floxed synectin knockin mice to generate synectin deletions in these cell types. Analysis of arterial circulation in hearts, kidneys, and skeletal muscles of EC-specific synectin mice demonstrated reduced numbers of arteries, reduced branching, and decreased arterial diameter, whereas no significant differences in these parameters were seen in smooth muscle–specific synectin knockout mice. These results were confirmed by analysis of arteriolar networks in the spinotrapezius muscle, where we also observed reduced arteriolar size and fewer artery-to-artery connections in EC-specific but not in SMC-specific synectin knockouts. Adult arteriogenesis, assessed as the ability to form new arteries in response to common femoral artery ligation, was also abnormal in Syn^{ECKO} but not Syn^{SMKO} mice. This was demonstrated both by the impaired blood flow recovery to the distal limb in Syn^{ECKO} mice and by the reduced numbers of small arteries forming above the knee.

All of these studies were performed using Tie2-Cre driver line, which, in addition to ECs, is also expressed in a small number of hematopoietic precursor cells that differentiate into several cell types, including monocytes/macrophages that play an important role in arterial morphogenesis. To exclude the possibility that Tie2 expression in cells other than ECs was responsible for the observed arteriogenesis defects, floxed synectin mice were also crossed with *Cdh5-CreERT2* transgenic mouse line that has a much more endothelium-restricted expression. Activation of Cdh5-driven Cre (iEC-SynKO), either during development or postnatally, reproduced the arterial morphogenesis defects observed in global synectin-null and Syn^{ECKO} mice, whereas angiogenesis (developmental and adult) was not affected.

As already alluded to, synectin regulates VEGFR2 signaling and, specifically, activation of ERK by ensuring, in partnership with neuropilin 1 and myosin VI, a rapid transit of VEGFR2 through the phosphatase zone, thus preventing its deactivation by phosphotyrosine phosphatase 1b.[33,53] Any reduction in endothelial ERK activation, as seen in synectin or myosin VI knockouts[31,32] or in Nrp1^{cyto} knockin mice,[33] results in arterial morphogenic defects. Interestingly, in all of these cases, as well as in the present study of endothelial-specific synectin deletion, angiogenesis remains normal.

The availability of synectin floxed mice has allowed us to address another critical point in arteriogenesis biology, namely the identification of the cell type critical to this process. The fact that endothelial disruption of synectin expression impairs all forms of arterial morphogenesis-developmental and adult as well as collateral development-clearly states that endothelial activation of ERK signaling, a process that synectin regulates, is central to arteriogenesis.

The nature of arteriogenic process, especially in adult tissues, has long remained poorly understood. The 2 most frequently advanced hypotheses are the remodeling of preexisting arterial vasculature into larger size arteries and de novo

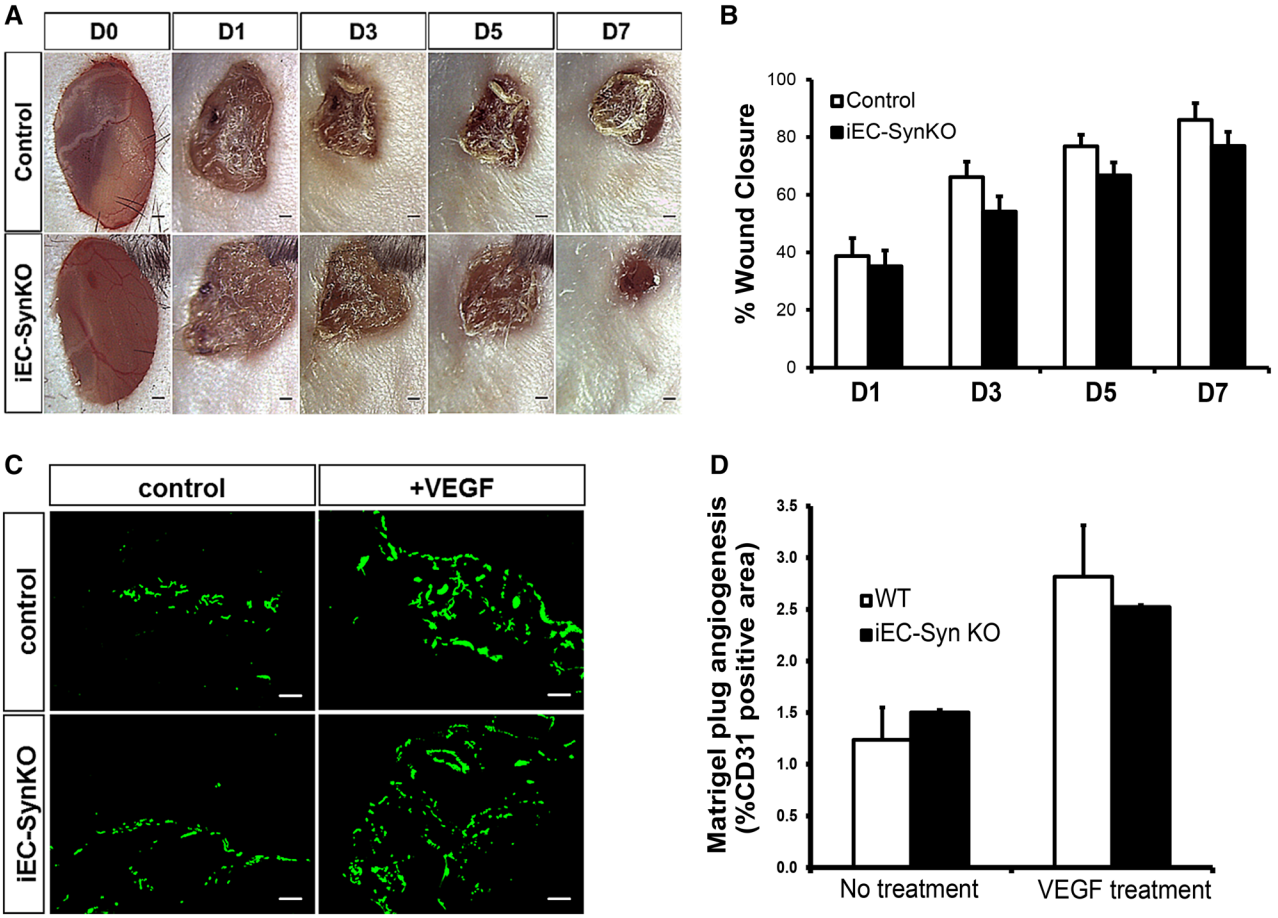

Figure 8. Adult angiogenesis is not affected in the induced endothelial synectin knockout (iEC-SynKO) mouse. A and **B**, Wounds were introduced in iEC-SynKO (Cdh5-Cre-ERT2) and littermate controls and imaged at the indicated times. Representative images of healing wounds are shown in (**A**), and quantification of the area of wound closure (mean±SEM) is shown in (**B**) (n=4 mice/group). **C** and **D**, Matrigel implants from iEC-SynKO (Cdh5-Cre-ERT2) and littermates controls. Representative images (**C**) and quantification (**D**) from CD31 immunolabeled Matrigel plug sections, with and without vascular endothelial growth factor (VEGF)-A165 treatment. Scale bar, 100 μm (n=3 mice/group). Syn indicates synectin; and WT, wild-type.

growth of new arteries. The remodeling of preexisting arteries (usually invoked in terms of collateral development, a special case of arteriogenesis) implies the expansion of the lumen and increased size of the vessel wall, a process that requires SMC proliferation.[19,54] In contrast, the de novo growth of new arteries suggests formation of new arterial conduits via arterialization of the capillary network. Such a process would be expected to be heavily dependent on EC proliferation because it requires capillary bed expansion.[12–14]

Defective arteriogenesis in EC-specific synectin mutants strongly argues for the second hypothesis. The decreased VEGF responsiveness of synectin-deficient endothelium likely affects arteriogenesis by affecting 2 critical processes: formation and expansion of vascular lumen and recruitment of mural cells. With regard to the former, it is interesting to note that in all cases of reduced endothelial ERK activation,[31–33] including the present study of EC-specific synectin deletion, arterial diameter for comparable arteries (eg, proximal coronary versus proximal coronary) is smaller than in control mice. Furthermore, in vitro assay demonstrates that reduced ERK activation leads to reduced lumen formation.[33] At the same time, excessive endothelial activation of ERK signaling leads to the formation of larger than normal diameter arteries.[55]

With regard to the latter, decreased endothelial synectin expression leads to reduced secretion of PDGF-BB,[36] the growth factor most associated with mural cell recruitment.[56,57] Combined, these 2 defects would lead to decreased capillary bed arterialization, a process that requires an increase in capillary lumen diameter and mural cell recruitment.

The role of synectin and endothelial VEGF resistance is supported by 2 other studies: (1) rescue of synectin-null arteriogenic defect by treatment with phosphotyrosine phosphatase 1b inhibitor, which abolishes the delayed VEGFR2 trafficking, thereby activating VEGR2/ERK signaling;[31,32] and (2) rescue of synectin-null and hypercholesterolemic mice (which are VEGF-resistant) by treatment with a phosphoinositol-3-kinase inhibitor, which activates ERK signaling independently of VEGFR2.[58] Although these studies were performed with global knockouts or globally impaired mice (hypercholesterolemia), the present study, with a selective endothelial knockout, closes the loop. Impaired VEGF signaling only in ECs is enough to affect arteriogenesis. This supports the de novo arteriogenesis rather than remodeling of preexisting collaterals as the dominant process.

In addition, we used a severe model of hindlimb ischemia that effectively eliminates any protective role of preexisting

collaterals. In fact, measurements of blood flow immediately after surgery demonstrate no difference between wild-type and synectin EC-null mice (iEC-SynKO, Syn^{ECKO}), supporting this argument. Also, the difference in blood flow recovery does not appear until day 7, a time course that is consistent with capillary bed arterialization that is largely endothelium-driven, whereas preexisting collateral growth typically peaks by day 3.[28,59] Therefore, all subsequent differences are largely because of de novo arteriogenesis, not because of preexisting collateral remodeling.

More broadly, endothelial resistance to VEGF signaling, whether because of defective VEGFR2 trafficking or because of other mechanisms, would be expected to result in arteriogenic defects. This concept is supported by many previous studies that addressed the role of VEGF signaling in the process of collateral formation.[5,17,29,30]

In conclusion, understanding how new arteries form in response to ischemia is crucial to developing effective treatments in ischemic vascular diseases. This study identifies ECs and endothelial VEGF responsiveness as key elements in growth and development of new arteries. We suggest that the focus of future therapeutics efforts should be on overcoming endothelial VEGF resistance frequently observed in patients with underlying pathologies such as atherosclerosis[28] and diabetes mellitus[60,61] and that simply providing additional VEGF either directly or via stimulation of mononuclear cell recruitment is unlikely to result in a therapeutic benefit.

Acknowledgments

We thank Steve N. Fiering (Dartmouth knockout core laboratory) for his help with generation of *gipc1*$^{flox/flox}$ mice; Rita Webber, Nicole Copeland, and Wayne D. Evangelisti (Yale Cardiovascular Research Center) for mouse colony management; Jiang Yifeng for micro-computed tomography angiography; John Bent for help with image editing; and Roa Harb for assistance with statistical analysis.

Sources of Funding

This work was supported, in part, by Brown-Coxe Foundation postdoctoral fellowship (F. Moraes), National Institutes of Health grant HL62289 (M. Simons), Leducq ARTEMIS Trans-Atlantic network grant (F. Moraes, M. Simons), and American Heart Association Beginning Grant-in-Aid 12BGIA12060154 (F.M. Gabhann).

Disclosures

None.

References

1. Potente M, Gerhardt H, Carmeliet P. Basic and therapeutic aspects of angiogenesis. *Cell*. 2011;146:873–887.
2. Carmeliet P, Jain RK. Molecular mechanisms and clinical applications of angiogenesis. *Nature*. 2011;473:298–307.
3. Geudens I, Gerhardt H. Coordinating cell behaviour during blood vessel formation. *Development*. 2011;138:4569–4583.
4. Chilian WM, Penn MS, Pung YF, Dong F, Mayorga M, Ohanyan V, Logan S, Yin L. Coronary collateral growth—back to the future. *J Mol Cell Cardiol*. 2012;52:905–911.
5. Toyota E, Warltier DC, Brock T, Ritman E, Kolz C, O'Malley P, Rocic P, Focardi M, Chilian WM. Vascular endothelial growth factor is required for coronary collateral growth in the rat. *Circulation*. 2005;112:2108–2113.
6. Eitenmüller I, Volger O, Kluge A, Troidl K, Barancik M, Cai WJ, Heil M, Pipp F, Fischer S, Horrevoets AJ, Schmitz-Rixen T, Schaper W. The range of adaptation by collateral vessels after femoral artery occlusion. *Circ Res*. 2006;99:656–662.
7. Resnick N, Einav S, Chen-Konak L, Zilberman M, Yahav H, Shay-Salit A. Hemodynamic forces as a stimulus for arteriogenesis. *Endothelium*. 2003;10:197–206.
8. Pipp F, Boehm S, Cai WJ, Adili F, Ziegler B, Karanovic G, Ritter R, Balzer J, Scheler C, Schaper W, Schmitz-Rixen T. Elevated fluid shear stress enhances postocclusive collateral artery growth and gene expression in the pig hind limb. *Arterioscler Thromb Vasc Biol*. 2004;24:1664–1668.
9. Herzog S, Sager H, Khmelevski E, Deylig A, Ito WD. Collateral arteries grow from preexisting anastomoses in the rat hindlimb. *Am J Physiol Heart Circ Physiol*. 2002;283:H2012–H2020.
10. Meier P, Gloekler S, Zbinden R, Beckh S, de Marchi SF, Zbinden S, Wustmann K, Billinger M, Vogel R, Cook S, Wenaweser P, Togni M, Windecker S, Meier B, Seiler C. Beneficial effect of recruitable collaterals: a 10-year follow-up study in patients with stable coronary artery disease undergoing quantitative collateral measurements. *Circulation*. 2007;116:975–983.
11. Chalothorn D, Faber JE. Strain-dependent variation in collateral circulatory function in mouse hindlimb. *Physiol Genomics*. 2010;42:469–479.
12. Simons M, Ware JA. Therapeutic angiogenesis in cardiovascular disease. *Nat Rev Drug Discov*. 2003;2:863–871.
13. Simons M. Angiogenesis: where do we stand now? *Circulation*. 2005;111:1556–1566.
14. Mac Gabhann F, Peirce SM. Collateral capillary arterialization following arteriolar ligation in murine skeletal muscle. *Microcirculation*. 2010;17:333–347.
15. Simons M. Chapter 14. Assessment of arteriogenesis. *Methods Enzymol*. 2008;445:331–342.
16. Cao R, Bråkenhielm E, Pawliuk R, Wariaro D, Post MJ, Wahlberg E, Leboulch P, Cao Y. Angiogenic synergism, vascular stability and improvement of hind-limb ischemia by a combination of PDGF-BB and FGF-2. *Nat Med*. 2003;9:604–613.
17. Clayton JA, Chalothorn D, Faber JE. Vascular endothelial growth factor-A specifies formation of native collaterals and regulates collateral growth in ischemia. *Circ Res*. 2008;103:1027–1036.
18. Murakami M, Simons M. Fibroblast growth factor regulation of neovascularization. *Curr Opin Hematol*. 2008;15:215–220.
19. Schaper W. Collateral circulation: past and present. *Basic Res Cardiol*. 2009;104:5–21.
20. Grunewald M, Avraham I, Dor Y, Bachar-Lustig E, Itin A, Jung S, Yung S, Chimenti S, Landsman L, Abramovitch R, Keshet E. VEGF-induced adult neovascularization: recruitment, retention, and role of accessory cells. *Cell*. 2006;124:175–189.
21. Ito WD, Arras M, Winkler B, Scholz D, Schaper J, Schaper W. Monocyte chemotactic protein-1 increases collateral and peripheral conductance after femoral artery occlusion. *Circ Res*. 1997;80:829–837.
22. Voskuil M, van Royen N, Hoefer IE, Seidler R, Guth BD, Bode C, Schaper W, Piek JJ, Buschmann IR. Modulation of collateral artery growth in a porcine hindlimb ligation model using MCP-1. *Am J Physiol Heart Circ Physiol*. 2003;284:H1422–H1428.
23. Robich MP, Matyal R, Chu LM, Feng J, Xu SH, Laham RJ, Hess PE, Bianchi C, Sellke FW. Effects of neuropeptide Y on collateral development in a swine model of chronic myocardial ischemia. *J Mol Cell Cardiol*. 2010;49:1022–1030.
24. Semenza GL. Regulation of tissue perfusion in mammals by hypoxia-inducible factor 1. *Exp Physiol*. 2007;92:988–991.
25. Patel TH, Kimura H, Weiss CR, Semenza GL, Hofmann LV. Constitutively active HIF-1alpha improves perfusion and arterial remodeling in an endovascular model of limb ischemia. *Cardiovasc Res*. 2005;68:144–154.
26. Skuli N, Majmundar AJ, Krock BL, Mesquita RC, Mathew LK, Quinn ZL, Runge A, Liu L, Kim MN, Liang J, Schenkel S, Yodh AG, Keith B, Simon MC. Endothelial HIF-2alpha regulates murine pathological angiogenesis and revascularization processes. *J Clin Inves*. 2012;122:1427–1443
27. Li J, Post M, Volk R, Gao Y, Li M, Metais C, Sato K, Tsai J, Aird W, Rosenberg RD, Hampton TG, Sellke F, Carmeliet P, Simons M. PR39, a peptide regulator of angiogenesis. *Nat Med*. 2000;6:49–55.
28. Tirziu D, Moodie KL, Zhuang ZW, Singer K, Helisch A, Dunn JF, Li W, Singh J, Simons M. Delayed arteriogenesis in hypercholesterolemic mice. *Circulation*. 2005;112:2501–2509.
29. Lloyd PG, Prior BM, Li H, Yang HT, Terjung RL. VEGF receptor antagonism blocks arteriogenesis, but only partially inhibits angiogenesis, in skeletal muscle of exercise-trained rats. *Am J Physiol Heart Circ Physiol*. 2005;288:H759–H768.
30. Jacobi J, Tam BY, Wu G, Hoffman J, Cooke JP, Kuo CJ. Adenoviral gene transfer with soluble vascular endothelial growth factor receptors impairs angiogenesis and perfusion in a murine model of hindlimb ischemia. *Circulation*. 2004;110:2424–2429.

31. Chittenden TW, Claes F, Lanahan AA, et al. Selective regulation of arterial branching morphogenesis by synectin. *Dev Cell*. 2006;10:783–795.
32. Lanahan AA, Hermans K, Claes F, Kerley-Hamilton JS, Zhuang ZW, Giordano FJ, Carmeliet P, Simons M. VEGF receptor 2 endocytic trafficking regulates arterial morphogenesis. *Dev Cell*. 2010;18:713–724.
33. Lanahan A, Zhang X, Fantin A, Zhuang Z, Rivera-Molina F, Speichinger K, Prahst C, Zhang J, Wang Y, Davis G, Toomre D, Ruhrberg C, Simons M. The neuropilin 1 cytoplasmic domain is required for VEGF-A-dependent arteriogenesis. *Dev Cell*. 2013;25:156–168.
34. Cai H, Reed RR. Cloning and characterization of neuropilin-1-interacting protein: a PSD-95/Dlg/ZO-1 domain-containing protein that interacts with the cytoplasmic domain of neuropilin-1. *J Neurosci*. 1999;19:6519–6527.
35. Dedkov EI, Thomas MT, Sonka M, Yang F, Chittenden TW, Rhodes JM, Simons M, Ritman EL, Tomanek RJ. Synectin/syndecan-4 regulate coronary arteriolar growth during development. *Dev Dyn*. 2007;236:2004–2010.
36. Paye JM, Phng LK, Lanahan AA, Gerhard H, Simons M. Synectin-dependent regulation of arterial maturation. *Dev Dyn*. 2009;238:604–610.
37. Xin HB, Deng KY, Rishniw M, Ji G, Kotlikoff MI. Smooth muscle expression of Cre recombinase and eGFP in transgenic mice. *Physiol Genomics*. 2002;10:211–215.
38. Koni PA, Joshi SK, Temann UA, Olson D, Burkly L, Flavell RA. Conditional vascular cell adhesion molecule 1 deletion in mice: impaired lymphocyte migration to bone marrow. *J Exp Med*. 2001;193:741–754.
39. Wang Y, Nakayama M, Pitulescu ME, Schmidt TS, Bochenek ML, Sakakibara A, Adams S, Davy A, Deutsch U, Lüthi U, Barberis A, Benjamin LE, Mäkinen T, Nobes CD, Adams RH. Ephrin-B2 controls VEGF-induced angiogenesis and lymphangiogenesis. *Nature*. 2010;465:483–486.
40. Claxton S, Kostourou V, Jadeja S, Chambon P, Hodivala-Dilke K, Fruttiger M. Efficient, inducible Cre-recombinase activation in vascular endothelium. *Genesis*. 2008;46:74–80.
41. Ray JL, Leach R, Herbert JM, Benson M. Isolation of vascular smooth muscle cells from a single murine aorta. *Methods Cell Sci*. 2001;23:185–188.
42. Jaba IM, Zhuang ZW, Li N, Jiang Y, Martin KA, Sinusas AJ, Papademetris X, Simons M, Sessa WC, Young LH, Tirziu D. No triggers rgs4 degradation to coordinate angiogenesis and cardiomyocyte growth. *J Clin Invest*. 2013;123:1718–1731.
43. Bailey AM, O'Neill TJ IV, Morris CE, Peirce SM. Arteriolar remodeling following ischemic injury extends from capillary to large arteriole in the microcirculation. *Microcirculation*. 2008;15:389–404.
44. Schneider CA, Rasband WS, Eliceiri KW. NIH Image to ImageJ: 25 years of image analysis. *Nat Methods*. 2012;9:671–675.
45. Tonnesen MG, Feng X, Clark RA. Angiogenesis in wound healing. *J Investig Dermatol Symp Proc*. 2000;5:40–46.
46. Peirce SM, Skalak TC. Microvascular remodeling: a complex continuum spanning angiogenesis to arteriogenesis. *Microcirculation*. 2003;10:99–111.
47. Tang Y, Harrington A, Yang X, Friesel RE, Liaw L. The contribution of the Tie2+ lineage to primitive and definitive hematopoietic cells. *Genesis*. 2010;48:563–567.
48. Hoefer IE, Grundmann S, van Royen N, Voskuil M, Schirmer SH, Ulusans S, Bode C, Buschmann IR, Piek JJ. Leukocyte subpopulations and arteriogenesis: specific role of monocytes, lymphocytes and granulocytes. *Atherosclerosis*. 2005;181:285–293.
49. Cochain C, Rodero MP, Vilar J, Récalde A, Richart AL, Loinard C, Zouggari Y, Guérin C, Duriez M, Combadière B, Poupel L, Lévy BI, Mallat Z, Combadière C, Silvestre JS. Regulation of monocyte subset systemic levels by distinct chemokine receptors controls post-ischaemic neovascularization. *Cardiovasc Res*. 2010;88:186–195.
50. Eichmann A, Simons M. VEGF signaling inside vascular endothelial cells and beyond. *Curr Opin Cell Biol*. 2012;24:188–193.
51. Simons M. An inside view: VEGF receptor trafficking and signaling. *Physiology (Bethesda)*. 2012;27:213–222.
52. Naccache SN, Hasson T, Horowitz A. Binding of internalized receptors to the PDZ domain of GIPC/synectin recruits myosin VI to endocytic vesicles. *Proc Natl Acad Sci U S A*. 2006;103:12735–12740.
53. Zhang X, Lanahan AA, Simons M. VEGFR2 trafficking: speed doesn't kill. *Cell Cycle*. 2013;12:2163–2164.
54. Cai WJ, Kocsis E, Wu X, Rodríguez M, Luo X, Schaper W, Schaper J. Remodeling of the vascular tunica media is essential for development of collateral vessels in the canine heart. *Mol Cell Biochem*. 2004;264:201–210.
55. Deng Y, Larrivée B, Zhuang ZW, Atri D, Moraes F, Prahst C, Eichmann A, Simons M. Endothelial RAF1/ERK activation regulates arterial morphogenesis. *Blood*. 2013;121:3988–96, S1.
56. Hellström M, Kalén M, Lindahl P, Abramsson A, Betsholtz C. Role of PDGF-B and PDGFR-beta in recruitment of vascular smooth muscle cells and pericytes during embryonic blood vessel formation in the mouse. *Development*. 1999;126:3047–3055.
57. Lindblom P, Gerhardt H, Liebner S, Abramsson A, Enge M, Hellstrom M, Backstrom G, Fredriksson S, Landegren U, Nystrom HC, Bergstrom G, Dejana E, Ostman A, Lindahl P, Betsholtz C. Endothelial PDGF-B retention is required for proper investment of pericytes in the microvessel wall. *Genes Dev*. 2003;17:1835–1840.
58. Ren B, Deng Y, Mukhopadhyay A, Lanahan AA, Zhuang ZW, Moodie KL, Mulligan-Kehoe MJ, Byzova TV, Peterson RT, Simons M. ERK1/2-Akt1 crosstalk regulates arteriogenesis in mice and zebrafish. *J Clin Invest*. 2010;120:1217–1228.
59. Heil M, Eitenmüller I, Schmitz-Rixen T, Schaper W. Arteriogenesis versus angiogenesis: similarities and differences. *J Cell Mol Med*. 2006;10:45–55.
60. Sasso FC, Torella D, Carbonara O, Ellison GM, Torella M, Scardone M, Marra C, Nasti R, Marfella R, Cozzolino D, Indolfi C, Cotrufo M, Torella R, Salvatore T. Increased vascular endothelial growth factor expression but impaired vascular endothelial growth factor receptor signaling in the myocardium of type 2 diabetic patients with chronic coronary heart disease. *J Am Coll Cardiol*. 2005;46:827–834.
61. Waltenberger J. VEGF resistance as a molecular basis to explain the angiogenesis paradox in diabetes mellitus. *Biochem Soc Trans*. 2009;37:1167–1170.

Novelty and Significance

What Is Known?

- Arterial occlusion results in the failure of blood delivery, leading to tissue ischemia.
- In some circumstances, blood flow can be re-established via the development of collateral vessels.
- Formation and growth of new arteries and collateral vessels are poorly understood processes.

What New Information Does This Article Contribute?

- Partial disruption of vascular endothelial growth factor receptor 2 signaling in endothelial cells impairs arteriogenesis, indicating that endothelial cells play a central role in arteriogenesis.
- These findings suggest a model of the de novo arteriogenesis in which arteries are formed by arterialization of the capillary bed, expansion of the vascular lumen, and recruitment of mural cells to form new arterial structures. This process is driven by endothelial cell responses to vascular endothelial growth factor.

Adult arteriogenesis is a physiologically important but poorly understood process. We examined the role of the endothelium in regulating arteriogenesis by specifically deleting synectin (*gipc1*), a protein involved in the regulation of vascular endothelial growth factor receptor 2 trafficking in endothelial and smooth muscle cells. We found that endothelium-specific deletion of synectin decreased arterial formation during embryonic development and reduced collateral formation in adult tissues. Together with previous studies that have demonstrated the involvement of synectin in vascular endothelial growth factor receptor 2 trafficking and activation of ERK signaling, our observations point to the key role of endothelium and, specifically, endothelial ERK signaling in regulating arteriogenesis. These results suggest that impaired endothelial responsiveness to vascular endothelial growth factor during conditions such as diabetes mellitus or atherosclerosis would attenuate arteriogenesis.

ENDOTHELIAL CELL-DEPENDENT REGULATION OF ARTERIOGENESIS

SUPPLEMENTAL MATERIAL

Mice

Mice homozygous for a conditional allele of synectin *(gipc1)* were generated by flanking exon 2 with *loxP* sites. Exon 2 contains the start codon for the synectin gene. A bacterial artificial chromosome (BAC) clone, containing the synectin genomic region, was obtained by screening the RPCl-22 129/SvEvTacBr BAC library (Genome Resource Facility at the Hospital for Sick Children). A 10kb *BstB I-Mfe I* fragment containing exon 2 was subcloned into pSMART LC Kan (Lucigen) plasmid vector for the construction of the targeting vector. A replacement targeting vector was constructed with the insertion of a loxP site into *BsrB I* restriction site upstream of exon 2, and the insertion of an Frt/loxP flanked neomycin cassette positioned 5' of exon 2, into the *PshAI* site downstream of exon2. The integrity of the construct was confirmed by restriction digestion and DNA sequencing. Using standard techniques previously described [1], targeted 129SvIMJ embryonic stem (ES) cells were generated and C57BL/6/129 SvIMJ mouse lines were developed from four positive ES cell clones. The presence of the targeted allele was identified by PCR and Southern blot. Three chimeras were born and bred to C57BL/6 mice, and F1 agouti offspring mice were genotyped by PCR to validate germline transmission.

The Frt-flanked neo gene was deleted *in vivo* by breeding gipc1 $^{flox/+}$ with the FLPeR (flipper) mice [2]. Offspring were backcrossed seven times into C57/Bl6 and genotyped by PCR. The *gipc1* ^{flox} allele was genotyped with primer pair Flox-*BsrBI-Fwd*: 5'AAGCAAAGGACAGTGCCAGT3', *BsrBI Rev*: 5'GGACCCACATACCTAGACTGC3'. Exon 2 was deleted by crossing the *gipc1*$^{flox/flox}$ mice with the Sm-MHC-Cre [3] , Tie2-Cre [4], Cdh5(PAC)-CreERT2 [5] and Pdgfbicre/ERT2[6] mice. *Gipc1*$^{flox/flox}$ animals were crossed with Sm-MHC-Cre mouse line and the progeny was bred to produce mice without synectin expression in smooth muscle cells (Syn^{SMKO}). To produce mice with endothelial-specific knockout of synectin, homozygous floxed synectin mice were crossed with the constitutive active Cre mouse line, Tie2-Cre (Syn^{ECKO}) and with the inducible Cre mouse lines (iEC-SynKO), *Cdh5-CreERT2* [5] and *Pdgf-*

icre/ERT2[6]. After established the different mouse lines, the genotyping was performed by Transnetyx (Cordova) using a quantitative real-time PCR-based (qPCR-based) system to detect the presence or absence of a target sequence within each sample. The animals were maintained in the Animal Research Center at Yale University. All animal experiments were performed under a protocol approved by the Institutional Animal Care and Use Committee (IACUC) of Yale University.

Tamoxifen injection

Induction of Cre expression in pups from was done by consecutive intragastric injections (P1-P3) of 100 ug of tamoxifen per pup. Induction of Cre expression in adult mice was done by 5 alternate day intra-gastric injections (P1-P9) and by other 5 alternate subcutaneous injections from (P11-P20) of 50ul/pup of tamoxifen (2mg/ml in corn oil).

Primary smooth muscle and endothelial cell isolation and culture

Primary smooth muscle cells (SMCs) were isolated as previously described [7] with minor modifications. In summary, the dorsal aorta was removed from adult mice and submerged in sterile PBS containing penicilin-streptomycin (100 I.U./ml penicillin:100 ug/ml streptomycin) and amphotericin B (2.5 µg/mL). The vessels were incubated in enzymatic digestion solution (Collagenase - 1mg/mL, Elastase-0.5mg/mL in media without serum) for 10min at 37ºC. After the first enzymatic digestion the vessels were stripped of adventitia and placed into new enzymatic solution for 1h at 37ºC, centrifuged and plated in culture medium (DMEM with 20% Fetal bovine serum, nonessential amino acids, sodium pyruvate, L-glutamine, and antibiotics at standard concentrations]). After 7–10 days, the cells began to migrate out from the tissue sections, reaching confluence in 15-20 days. The cells were harvested and protein lysates extracted to undergo western blotting in order to check synectin protein levels. Primary endothelial cells were isolated from the heart and lung of adult mice using a previously described protocol [8, 9]. In summary, the tissues (heart and lung) of 4 mice/group were harvested, minced finely with scissors and then digested in 25ml collagenase 0.2% (w/v) at 37^{o}C for 45 min. The cells were pelleted and resuspended in DMEM-

20% FBS. The cell suspension was incubated, with rotation, with PECAM-1-coated beads (Invitrogen) at room temperature for 20min. Using a magnetic separator, the bead-bound cells were recovered, washed with DMEM-20%FBS, suspended in 10ml complete culture medium (same as described above used for smooth muscle cell culture but complemented with 100ug/ml heparin, 100ug/ml ECGF growth supplement [ECGF: Biomedical Technologies, Stoughton, MA]) , and finally plated in a gelatin-coated 10cm tissue culture dish.

Western blotting

Cells were washed with PBS and lysed in RIPA buffer with protease (Sigma) and phosphatase (Bioproducts) inhibitors. The cell lysate was used for western blot. Equal amounts of protein were loaded in 12% ReadyGels (Bio-Rad), separated and transferred at constant voltage.

Reagents and Antibodies

The following antibodies were used in the study: mouse monoclonal αSMA clone 1A4 (#A2547, Sigma), goat polyclonal anti-VE-cadherin (#SC6458,Santa Cruz), rabbit polyclonal anti-synectin (courtesy Dr. A. Horowitz), anti- phospho-VEGF Receptor 2 (Tyr1175 #2478, Cell Signaling), anti-total VEGFR-2 (#2479, Cell Signaling) anti-phospho p44/42 MAP Kinase (phospho-ERK, #9106, Cell Signaling), anti-p44/42 MAP Kinase (total ERK, #9102, Cell Signaling). The growth factors, PDGF-BB (220-BB) and VEGF-A165 (293-VE) were obtained from R&D Systems.

RNA isolation and RT-PCR

Total RNA was extracted from Syn^{SMKO} carotid artery and aortas and from iEC-SynKO lungs, using RNeasy plus Mini Kit (Qiagen), cDNA synthesis was performed with iScript cDNA Synthesis kit (BioRad) and PCR amplification (RT-PCR) was performed with synectin specific primers:

LSyn (1-2): 5'CAGGTCTCCCAGCCAGAGT3'

RSyn (1-2): 5'GTAGTCGGAAGGCCTCAGC 3'

Quantitative real time PCR (qRT-PCR) was used to measure synectin expression in iEC-SynKO lungs and in Syn^{ECKO} endothelial cells (data not shown). SYBR GREEN Mastermix (BioRAD) and Bio-Rad CFX94 detection system were used. Data were normalized to endogenous VE-Cadh primers shown in the table below and confirmed with commercial available primers from Qiagen (VE-Cadh #QT01052044).

List of primers used for qPCR:

*L(VeCadh)*q	ATTGAGACAGACCCCAAACG
*R(VeCadh)*q	TTCTGGTTTTCTGGCAGCTT
*Lsyn(ex1-2)*q	AGTTTCGAGAGGACCGAGCA
Rsyn(ex1-2)q	CCTCCTCATTTCCACCAGA
*LSyn (ex2)*q	GCAGCAGGAGAATCCCAGAT
*RSyn (ex2)*q	GCCGTACAGCTCCTTGACAT

Hindlimb Ischemia Model

Surgical hindlimb ischemia

This was done as previously described by our lab [8, 10]. Briefly, surgical procedures were performed in mice under anesthesia and sterile conditions. A vertical longitudinal incision was made in the right hindlimb (10 mm long). The right femoral artery and its side branches were dissected and ligated with 6 – 0 silk sutures spaced 5 mm apart, and the arterial segment between the ligatures was excised.

Assessment of Blood Perfusion by Laser-Doppler flow-Imaging (LDI)

Measurement of blood flow was done by scanning both rear paws with a LDI analyzer (Moor Infrared Laser Doppler Imager Instrument, Wilmington, Delaware) before and after the surgical procedure (days 0, 3, 7, and 14). The animal was kept under 1% isoflurane anesthesia and its body temperature was strictly maintained between 36.5°C- 37.5°C as previously described [8, 10, 11]. Low or no perfusion is displayed as dark blue, whereas the highest degree of perfusion is displayed as red. The images obtained were quantitatively converted into histograms with Moor LDI processing software V3.09. Data were reported as the ratio of flow in the right/left (R/L) hindlimb and calf regions (not shown). Measurement of blood

flow was done before and after the surgical procedure (days 0, 3, 7, and 14).

For Syn^{SMKO} and Syn^{ECKO} mouse lines, 10 mutant and 9 control 10-12 week old females were used. For iEC-SynKO mouse line, 6 mutant and 6 control 10 week old males were used.

Micro-CT Angiography

For microcomputed tomography (mCT) of the cardiac, renal and hindlimb vasculature, euthanized mice were injected with 0.7ml solution (bismuth contrast solution) in the descending aorta. The mice were immediately chilled in ice and immersion fixed in 2% paraformaldehyde overnight. The vasculature was imaged and quantified as described previously [8, 10] and in detail as follows: 2D mCT scans were acquired with a *GE eXplore* Micro-CT System (GE Healthcare) **,** using a 400 cone-beam filtered back projection algorithm, set to an 8-27-μm micron slice thickness. Micro-CT quantification was done as previously described [12].In brief, data were acquired in an axial mode, covering a volume of 2.0 cm in the z direction with a 1.04-cm field of view. During post-processing, a 40 000 gray-scale value was set as a threshold to eliminate noise (air, water, and bone signals) with minimal sacrifice of vessel visualization. The mCT data were processed using real time 3D volume rendering software (version 3.1, Vital Images, Inc. Plymouth, MN) and microview (version 1.15, GE medical system) software to reconstruct three 2D maximum-intensity projection images (x, y,and z axes) from raw data. Quantification was performed using a modified Image ProPlus 5.0 algorithm (Media Cybernatics). The data are expressed as vessel number, representing total number of vessels, of specified diameter counted in 200 z sections from thigh and kidney or in 350-400 z sections from heart images. For analysis of heart and kidney, and hindlimb vasculature, 4-5 mutant mice and 4 gender and age matched controls were used.

Harvest and staining of whole mount tissues

Spinotrapezius staining and analysis

Mouse spinotrapezius tissues were extracted as described previously [13, 14]. Briefly, the dorsal skin was

opened and the dorsal shoulder fat pad bisected to expose the spinotrapezius muscle. The superficial muscle was separated from the deeper-lying latissimus dorsi, stripped of fascia and cut at the cranial and medial edges for removal. Tissues were washed in PBS, permeabilized in blocking solution (1% BSA, 0.5% TWEEN-20 in PBS) for 4hours at room temperature (RT) and labeled with smooth muscle α-actin antibody (1A4-Cy3, 1:200) and lectin (IB4-Alexa488, 1:100) at RT for one hour and overnight at 4°C. The samples were washed in PBS and whole-mounted on slides for imaging.

Pseudocoloring of arterioles was performed using intensity filters, and confirmed by inspection. Complete maps of the spinotrapezius arterial networks were acquired at micron-resolution by stitching together 20-25 images (each image with 1.85 um/pixel), acquired by fluorescent microscopy (Nikon 80i Microscope). Quantification of vessel diameters was done using ImageJ software [15]. Diameters were measured at (a) the points where the feed arteries entered the spinotrapezius muscle ("input arterioles") and (b) the set points of narrowest diameter ("bottlenecks"- not shown) in the parallel collateral arteriole pathways between the input arterioles. The data are expressed as the diameters of the input arterioles and the number of collateral arcades in these muscles.

Retina Staining

The eyes were removed from neonates at postnatal day 5 (P5) and 17 (P17) and prefixed in 4% paraformaldehyde (4%PFA) for 15min at room temperature. The transgenic mouse line Pdgfb-icre/ERT2-IRES-EGFP [6] allows detection of Cre recombination activity by assessing GFP expression. Therefore, dissected retinas from Pdgf-icre/ERT2;Syn^{FF} neonates were immediately inspected for GFP expression and iEC-SynKO were screened from the control littermates.

The dissected retinas were blocked overnight at 4° C in TNBT (0.1M Tris-HCl, 150 mM NaCl, 0.2% blocking reagent [PerkinElmer] supplemented with 0.5% TritonX-100). After washing, the retinas were incubated with IsolectinB4, Alexa Fluor® 488 Conjugate (Molecular Probes CatN#I21411) in Pblec (1 mM MgCl2, 1 mM CaCl2, 0.1 mM MnCl2, 1% Triton X-100 in PBS) for 2 hours at RT, P17 retinas were also stained with smooth muscle α-actin (SMA, IA4-Cy3 #C6198, Sigma). The retinas were washed 6

times, for 10min in PBS, fixed briefly for 5min in 4%PFA, washed twice in PBS and mounted in fluorescent mounting medium (DAKO, Carpinteria, CA, USA). Three mutant iEC-SynKO (*Pdgf-icre/ERT2)* mice and 3 control littermates as well as 4 mutant Syn^{ECKO} (*Tie2-cre)* mice and 4 control littermates were used for phenotypic analysis under a fluorescent microscope. Low and high magnification images were acquired using fluorescent (Nikon 80i Nikon Ti-E Eclipse inverted microscope) and confocal (ZEISS LSM710 laser scanning confocal) microscopes. Quantification was performed in iEC-SynKO neonates; 20-25 images per group were acquired and Biological CMM Analyzer software[16] was used to quantify vascular area and number of vessel branch points per image.

Adult angiogenesis models

In vivo matrigel assay

The growth factor reduced Matrigel (BD Bioscience) was thawed on ice, one day before procedure. The matrigel was pre-mixed with heparin (5U) with or without VEGF-A 165 (100ng/ml) and injected into subcutaneous tissues of 12-week old male mice from iEC-SynKO mouse line (*Cdh5-CreERT2*). After 7 days from injection, matrigel plugs were recovered from the sacrificed mice, embedded in OCT and cryosectioned in 10um sections.

To identify infiltrating endothelial cells, the sections were stained with anti-CD31 antibody (BD pharmingen TM) and random images from each plug were acquired by fluorescent microscopy. CD31-positive vessels were quantified using ImageJ v1.47g software and expressed as a read out of angiogenesis. Three mutant mice and 3 control littermates were used for the analysis.

Wound healing model

Wound healing assays were performed by the back punch model. In this model a wound is created in the back skin (6-mm punch) and the healing process is analyzed over time. The rate of wound closure is dependent on angiogenesis.[17] Before surgery, mice were anaesthetized by intraperitoneal injection of ketamine (100mg/kg)/xylazine (10mg/Kg) solution. The fur was removed from the surgical site and the skin was cleaned with ethanol. Full thickness wounds were made with a sterile 6mm biopsy punch in the

back skin (Miltex, # 33-36), keeping the underlying muscle intact. Images of the wounds were acquired with a LEICA M125 microscope with a HC80 HD camera (Leica Germany) and ImageJ v1.47g software was used to quantify wound sizes. Measure of the wound diameter was done at 0, 1, 3, 5 and 7 days after procedure and is shown as a percentage of the original wound. Four mutant mice and 4 control littermates were used for the analysis (12-14 wks, males).

Statistical analysis

Data are presented as mean ±SEM. Comparisons between 2 independent groups were performed with a 2-sample t-test. Differences were considered statistically significant if $p \leq 0.05$. Differences between multiple groups were assessed with 2-way ANOVA followed by the post-hoc Tukey's HSD multiple comparisons test.

1. Lathrop MJ, Chakrabarti L, Eng J, Rhodes CH, Lutz T, Nieto A, Liggitt HD, Warner S, Fields J, Stoger R, Fiering S. Deletion of the chd6 exon 12 affects motor coordination. *Mamm Genome*. 2010;21:130-142
2. Farley FW, Soriano P, Steffen LS, Dymecki SM. Widespread recombinase expression using flper (flipper) mice. *Genesis*. 2000;28:106-110
3. Xin HB, Deng KY, Rishniw M, Ji G, Kotlikoff MI. Smooth muscle expression of cre recombinase and egfp in transgenic mice. *Physiol Genomics*. 2002;10:211-215
4. Koni PA, Joshi SK, Temann UA, Olson D, Burkly L, Flavell RA. Conditional vascular cell adhesion molecule 1 deletion in mice: Impaired lymphocyte migration to bone marrow. *The Journal of experimental medicine*. 2001;193:741-754
5. Wang Y, Nakayama M, Pitulescu ME, Schmidt TS, Bochenek ML, Sakakibara A, Adams S, Davy A, Deutsch U, Luthi U, Barberis A, Benjamin LE, Makinen T, Nobes CD, Adams RH. Ephrin-b2 controls vegf-induced angiogenesis and lymphangiogenesis. *Nature*. 2010;465:483-486
6. Claxton S, Kostourou V, Jadeja S, Chambon P, Hodivala-Dilke K, Fruttiger M. Efficient, inducible cre-recombinase activation in vascular endothelium. *Genesis*. 2008;46:74-80
7. Ray JL, Leach R, Herbert JM, Benson M. Isolation of vascular smooth muscle cells from a single murine aorta. *Methods Cell Sci*. 2001;23:185-188
8. Chittenden TW, Claes F, Lanahan AA, Autiero M, Palac RT, Tkachenko EV, Elfenbein A, Ruiz de Almodovar C, Dedkov E, Tomanek R, Li W, Westmore M, Singh JP, Horowitz A, Mulligan-Kehoe MJ, Moodie KL, Zhuang ZW, Carmeliet P, Simons M. Selective regulation of arterial branching morphogenesis by synectin. *Developmental cell*. 2006;10:783-795
9. Li J, Shworak NW, Simons M. Increased responsiveness of hypoxic endothelial cells to fgf2 is

mediated by hif-1alpha-dependent regulation of enzymes involved in synthesis of heparan sulfate fgf2-binding sites. *J Cell Sci*. 2002;115:1951-1959
10. Tirziu D, Moodie KL, Zhuang ZW, Singer K, Helisch A, Dunn JF, Li W, Singh J, Simons M. Delayed arteriogenesis in hypercholesterolemic mice. *Circulation*. 2005;112:2501-2509
11. Zhuang ZW, Shi J, Rhodes JM, Tsapakos MJ, Simons M. Challenging the surgical rodent hindlimb ischemia model with the miniinterventional technique. *Journal of vascular and interventional radiology : JVIR*. 2011;22:1437-1446
12. Simons M. Chapter 14. Assessment of arteriogenesis. *Methods in enzymology*. 2008;445:331-342
13. Bailey AM, O'Neill TJt, Morris CE, Peirce SM. Arteriolar remodeling following ischemic injury extends from capillary to large arteriole in the microcirculation. *Microcirculation*. 2008;15:389-404
14. Mac Gabhann F, Peirce SM. Collateral capillary arterialization following arteriolar ligation in murine skeletal muscle. *Microcirculation*. 2010;17:333-347
15. Schneider CA, Rasband WS, Eliceiri KW. Nih image to imagej: 25 years of image analysis. *Nature methods*. 2012;9:671-675
16. Jones EA, Yuan L, Breant C, Watts RJ, Eichmann A. Separating genetic and hemodynamic defects in neuropilin 1 knockout embryos. *Development*. 2008;135:2479-2488
17. Tonnesen MG, Feng X, Clark RA. Angiogenesis in wound healing. *The journal of investigative dermatology. Symposium proceedings / the Society for Investigative Dermatology, Inc. [and] European Society for Dermatological Research*. 2000;5:40-46